



Full Length Article

Fuel gas production through waste polyethylene gasification using bauxite residue as the oxygen carrier

Xudong Du^a, Jun Wang^a, Jiaying Song^a, Yuhan Pan^a, Jingyuan Sima^a, Chenxi Zhu^a, Huaping Gao^b, Linlin Guo^c, Jie Zhang^c, Qunxing Huang^{a,*}

^a State Key Laboratory of Clean Energy Utilization, Institute for Thermal Power Engineering, Zhejiang University, Hangzhou 310027, China

^b Faculty of Environmental Science and Engineering, Kunming University Of Science And Technology, Kunming 650000, China

^c China Energy Conservation and Environmental Protection Group, Linyi 276000, China



ARTICLE INFO

Keywords:

Fuel gas
Bauxite residue
Waste plastic
Oxygen carrier
Gasification

ABSTRACT

In this study, waste polyethylene (PE) was gasified to produce alternative gas fuel using bauxite residue (BR) as an oxygen carrier in a two-stage reactor. PE was pyrolyzed in the first stage, and the volatiles were subsequently gasified with BR. The influences of temperature and mass ratio on the fuel gas composition were determined. The experimental results indicated that a higher temperature benefits gas production. The gas yield was 0.714 Nm³/kg at 850 °C, and the CH₄ yield was 0.231 Nm³/kg. Increasing the BR mass ratio (Fe₂O₃ to fuel) could lead to over-oxidization (combustible gas production values were 0.531 Nm³/kg and 0.503 Nm³/kg at ratios of 1:2 and 1:4, respectively). Compared with the traditional oxygen carrier Fe₂O₃, BR showed a stronger oxygen release capability. The oxygen efficiency of BR was over 100% higher than that of Fe₂O₃. Moreover, the three-stage reactor improved the quality of gas (gas yield was 0.771 Nm³/kg and the production of H₂, CH₄, and CO accounted for 33.425%, 31.349%, and 19.186%, respectively) compared to the two-stage reactor. Furthermore, the Fe contained in the BR was reduced to Fe₃O₄, which might have contributed to the magnetic separation. Therefore, the results offer a promising method for the efficient utilization of waste plastic and BR.

1. Introduction

Plastic, as an emerging high polymer material, has widely become a good substitute for traditional materials such as paper and ceramics in various industries because of its light weight, high strength, good insulation, and good transparency since its discovery in the 1900 s [1,2]. According to Eurostat, in 2019, global plastic production was approximately 368 million tons, and polyethylene (PE) accounted for the highest proportion (29.8%) [3]. However, the service life of plastic materials is limited. Most plastic products become “white waste” in a year [4], and the packaging plastic is discarded after a single use. Meanwhile, plastic requires hundreds of years to degrade naturally in the environment because of its stable structure. The rapid production and consumption of plastic have caused serious problems. Currently, plastic pollution is regarded as a global problem [5]. The most common treatments for plastic waste are landfills and incineration, which release large quantities of various pollutants [6,7]. Moreover, a large amount of CO₂ is generated during incineration, which exacerbates the greenhouse

effect. In recent years, considerable efforts have been made in low-carbon and sustainable technologies to mitigate climate change and control carbon dioxide emissions [8]. Plastics have extremely high volatile matter and can be easily decomposed at high temperatures. Additionally, the main components of plastic are carbon and hydrogen, which can be converted into CO and H₂. Consequently, the application of plastic for fuel gas production is a feasible low-carbon sustainable technology. In industrial applications, syngas is generated by the limited oxidation (air or pure oxygen as oxidants) of fuel. However, nitrogen in the air may dilute the gas generated during the reaction, and the use of pure oxygen increases the cost [9]. Thus, applying an oxygen carrier is an ideal method for the gasification process. The lattice oxygen in the oxygen carrier was used for the partial oxidation to avoid the dilution problem. Moreover, some types of industrial wastes [10,11] and natural ores [12,13] can also be used as oxygen carriers, and their cost can be easily controlled.

Generally, oxygen carriers can be classified as Fe-based [14], Ni-based [15], Cu-based [16], Mn-based [17,18] and Co-based [19]

* Corresponding author.

E-mail address: hqx@zju.edu.cn (Q. Huang).

<https://doi.org/10.1016/j.fuel.2022.123878>

Received 27 November 2021; Received in revised form 19 February 2022; Accepted 12 March 2022

Available online 5 April 2022

0016-2361/© 2022 Elsevier Ltd. All rights reserved.

materials. Among these, Fe-based materials have attracted wide attention owing to their low cost and environmentally friendly characteristics [14]. Cuadrat A et al. applied ilmenite as oxygen carrier in a 500 W_{th} continuous unit, no decrease on the oxygen transport capacity of ilmenite was found after 35 h operation [20]. Zhang S et al. modified the iron ore oxygen carrier with biomass ash and achieved stable CO₂ content at 94.56% in a 1 kW continuous reactor [21]. However, traditional Fe-based oxygen carriers can sinter easily at high temperatures. Therefore, Al₂O₃ [22], SiO₂ [23], and TiO₂ [24] were used to enhance the reaction performance of Fe-based oxygen carriers. As a waste generated in the aluminum industry [25], bauxite residue (red mud) is a complex mixture of Fe₂O₃, CaO, Al₂O₃, SiO₂, and TiO₂, thereby making it feasible for oxygen carrier applications. As reported, 1–2.5 tons of bauxite residue will be generated for every ton of produced alumina [26]. According to the data, by 2015, the global bauxite residue reserve reached nearly 4,000 million tons and still continuous to increase [27]. The efficient and environmentally friendly application of bauxite residue is a major concern. Apart from being used as building materials [28,29], raw materials for extraction [30] and synthetic pigments [31], bauxite residue is also a potential low-cost oxygen carrier because of its high iron content and unique composition.

At present, the role of bauxite residue in pyrolysis, combustion, and other thermochemical conversion processes have been studied by researchers. Gu et al. found that the alkali metal in the bauxite residue enhanced the chemical looping combustion of coal [12]. Lin et al. doped MgO and NiO into bauxite residue as the oxygen carrier, and achieved higher CO₂ selectivity (99%) and CH₄ conversion (65%–75%) [32]. López et al. discovered that bauxite residue has a certain activity in plastic pyrolysis [33]. Bao et al. evaluated the effect of various inert supports and indicated that Al₂O₃ and SiO₂ contributed to the stability of the bauxite residue, and TiO₂ was important in providing strong mechanical strength to the bauxite residue oxygen carriers [34]. Mendiara T et al. investigated the behavior of bauxite waste material as oxygen carrier and obtained high combustion efficiency up to 90% in a continuous 500 W_{th} CLC unit [35]. Abad A et al. found that the total oxygen demand of red mud was lower than that of ilmenite with Bituminous coal as fuel in the 0.5 kW_{th} CLC unit [36]. Although bauxite residue is a promising oxygen carrier for the gasification of plastic, there has been limited systematic study regarding this.

In this work, bauxite residue was used as the oxygen carrier for the gasification of PE under different reaction conditions (temperature and mass ratio). The gas was analyzed by gas chromatography (GC) to determine its composition. Quantitative calculations were conducted to determine the gas production. Moreover, the reaction activity of the bauxite residue was compared to that of pure Fe₂O₃. Different characterization methods (X-ray fluorescence, X-ray diffraction, scanning electron microscopy, and N₂ adsorption/desorption isotherms) were applied to explore the composition and surface properties of the bauxite residue. Additionally, the experimental equipment was modified with an additional reaction stage to improve the gas yield and obtain more CH₄, H₂, and CO. This work was aimed at applying bauxite residue and waste plastics for the gasification process to produce high-quality fuel gas and reduce the bauxite residue. The one-step recovery technique of waste plastic and bauxite residue provides an innovative method for waste recycling.

2. Material and experimental methods

2.1. Material

Typical bauxite residue (BR) was obtained from Yunnan Wenshan Aluminum Co., Ltd., and its composition was analyzed by X-ray fluorescence (XRF; Shimadzu XRF-1800, Japan), and the results are presented in Table 1.

The BR was pretreated with deionized water until it reached a pH ≤ 8, and was then dried at 105 °C for 48 h. After drying, the BR was

Table 1
Composition of raw BR (dry basis).

Component	Fe ₂ O ₃	CaO	Al ₂ O ₃	SiO ₂	Na ₂ O	TiO ₂	Balance
Content (%)	26.97	21.62	21.16	12.66	7.06	5.33	5.19

calcined at 900 °C for 2 h in air to completely oxidize the iron to Fe₂O₃. Subsequently, the samples were ground to less than 0.25 mm (60 mesh).

The PE sample was purchased from Meisheng Engineering Plastics Company (China, purity: 99%), with an average diameter of 0.01 mm. The quartz sand (SD; 0.125–0.08 mm, 120–180 mesh) and Fe₂O₃ used were purchased from China Shanghai Macklin Biochemical Technology Co., Ltd.

2.2. Characterizations

X-ray diffraction (XRD) of BR was conducted using an X-pert Powder diffractometer (PANalytical, Netherlands) with a scanning range (2θ) of 10–90° and at a scanning speed of 2°/min.

Scanning electron microscopy (SEM, Sigma 300, Germany) was used to observe the surface morphology of the BR before and after the reactions.

N₂ adsorption/desorption isotherms were obtained using an APSA 2460 (Micromeritics, America) automatic surface area and pore size analyzer, and the samples were degassed at 300 °C for 10 h before testing.

2.3. Experimental setup

As shown in Fig. 1, the experimental apparatus mainly comprises a quartz reactor with two sections of different diameters and an electric furnace. The inner diameters of the two sections were 41 mm and 26 mm, respectively. PE is pyrolyzed in a quartz boat placed in section 1 under a N₂ atmosphere. The reaction section is described as section 2. The pyrolysis gases reacted with the oxygen carrier. An electric furnace (SKF-2–13 Hangzhou Blue Sky Instrument Co., Ltd., China) supplied heat to maintain the reaction temperature at 650 °C, 750 °C, 850 °C, and 900 °C. The experimental conditions are presented in Table 2.

Prior to the reaction, N₂ was used to remove air from the device. When purging was completed, the mass flow of N₂ was set at 100 mL/min and maintained until the end of the experiments (the reacted oxygen carrier was also cooled to 20–25 °C under the protection of N₂). Subsequently, PE was transferred to section 1 for pyrolysis. The generated pyrolysis gases left section 1 and entered section 2, and were carried by N₂. Thereafter, the high-temperature gas was passed through an ice bath to retain condensable products. The gas was collected in 5 L gas bags and analyzed by GC (Agilent 490 Micro GC) with thermal conductivity (TCD) detectors and three separate packed-columns (MS5A 10 m column at 80 °C, PPU 10 m hold at 80 °C, and 10 m Al₂O₃/KCl column at 100 °C). Every experiment would last 20 min with 0.5 g PE input. The experiment details are listed in Table S3.

3. Result and discussion

3.1. General evaluation for the gasification performance

The indicators for evaluating the results of the experiments are as follows: gas composition, lower heating value (LHV), total gas production (TGP), combustible gas production (CGP), effective component production of plastic syngas (H₂, CH₄, and CO) (EGP), carbon conversion efficiency (CCE), hydrogen conversion efficiency (HCE), and oxygen efficiency (OE):

$$TGP(Nm^3/kg) = \sum V(gas) \quad (1)$$

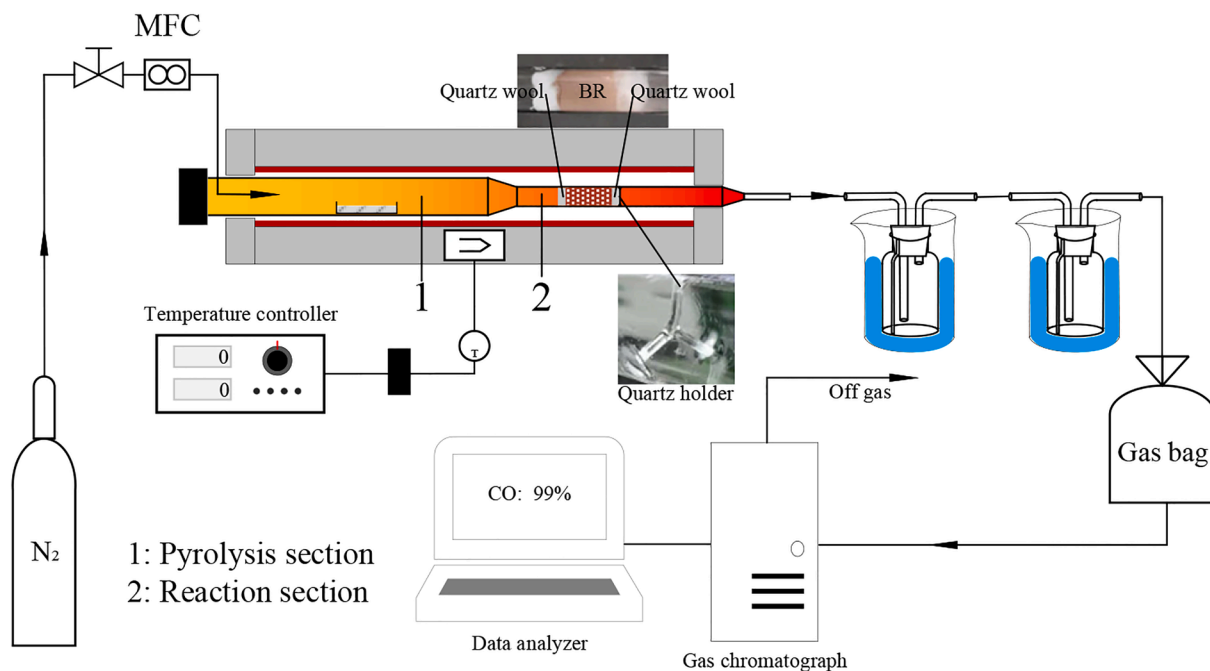


Fig. 1. Schematic diagram of the experimental system(MFC: mass flow controller).

Table 2
Conditions of the experiments.

Experiment conditions	Oxygen carrier	Temperature 1 (°C)	Temperature 2 (°C)	Temperature 3 (°C)	Mass ratio (PE:Fe ₂ O ₃)
BR6502	BR	650	650	not adopted	1:2
BR7502	BR	750	750	not adopted	1:2
BR8502	BR	850	850	not adopted	1:2
BR7504	BR	750	750	not adopted	1:4
SD650	SD	650	650	not adopted	1:0
SD750	SD	750	750	not adopted	1:0
SD850	SD	850	850	not adopted	1:0
FE7502	Fe ₂ O ₃	750	750	not adopted	1:2
BR2	BR-BR	850	850	900	1:2-1:1

$$CGP(Nm^3/kg) = TGP - V(CO_2) \quad (2)$$

$$EGP(Nm^3/kg) = V(H_2) + V(CO) + V(CH_4) \quad (3)$$

$$CCE(\%) = \frac{C(gas)}{C(fuel)} \times 100\% \quad (4)$$

$$HCE(\%) = \frac{H(gas)}{H(fuel)} \times 100\% \quad (5)$$

$$OE(\%) = \frac{O(gas)}{O(OCs)} \times 100\% \quad (6)$$

where $V(CO_2)$, $V(H_2)$, $V(CO)$, and $V(CH_4)$ are the volumes of CO_2 , H_2 , CO , and CH_4 , respectively. $C(gas)$ and $C(fuel)$, and $H(gas)$ and $H(fuel)$ correspond to the total carbon and total hydrogen in the gas production or fuel, respectively. $O(gas)$ and $O(OCs)$ correspond to the total oxygen in the fuel and oxygen carrier, respectively, which are used in each test.

3.2. Gas analysis

The compositions and yields of the gas products were calculated and are listed in Table S2. Overall, the LHV of the fuel gas ranges from 18.245 MJ/Nm³ to 57.283 MJ/Nm³. The CGP and EGP of BR2 reached their highest values of 0.659 and 0.647 Nm³/kg, respectively, and also led to the best TGP of 0.771 Nm³/kg. And it's worth noting that all the

results of gas are nitrogen and water free.

3.3. Effects of oxygen carriers in the gasification process

The results for SD750, FE7502, and BR7502 are shown in Fig. 2. Experiments were conducted at 750 °C. The addition of an oxygen carrier promotes the production of small molecules (H_2 , CO , CO_2 , and CH_4). As shown in Fig. 2(a), the yields of H_2 , CH_4 , and CO increased after the application of oxygen carriers. The production of CO_2 also increased to 0.039 (FE7502) and 0.089 Nm³/kg (BR7502) because of over-oxidation. However, BR exhibits a better promoting effect on the formation of small molecular products compared to Fe_2O_3 . The yields of H_2 , CO , CO_2 , and CH_4 of BR7502 were higher than those of FE7502. However, there are some differences between BR and Fe_2O_3 regarding the influence of macromolecular gas products. The formation of C_2H_4 , C_2H_6 , and C_3H_6 is promoted by the pure Fe_2O_3 oxygen carrier at 750 °C compared to that of SD750. However, a weaker promotion effect was shown by BR at the same temperature. The production of C_2H_6 and C_3H_6 is inhibited, and may be attributed to the stronger oxidizability of BR.

In Fig. 2(b), the combined outputs of H_2 , CH_4 , CO , and CO_2 increase from 40.764% (SD750) to 47.542% (FE7502) and 57.240% (BR7502), respectively. This demonstrates that smaller molecules tend to be generated. Although the percentage contents of H_2 and CH_4 increased insignificantly after the addition of BR and Fe_2O_3 , their quantitative yields increased. The relative content of C_2H_4 of SD750 reached its

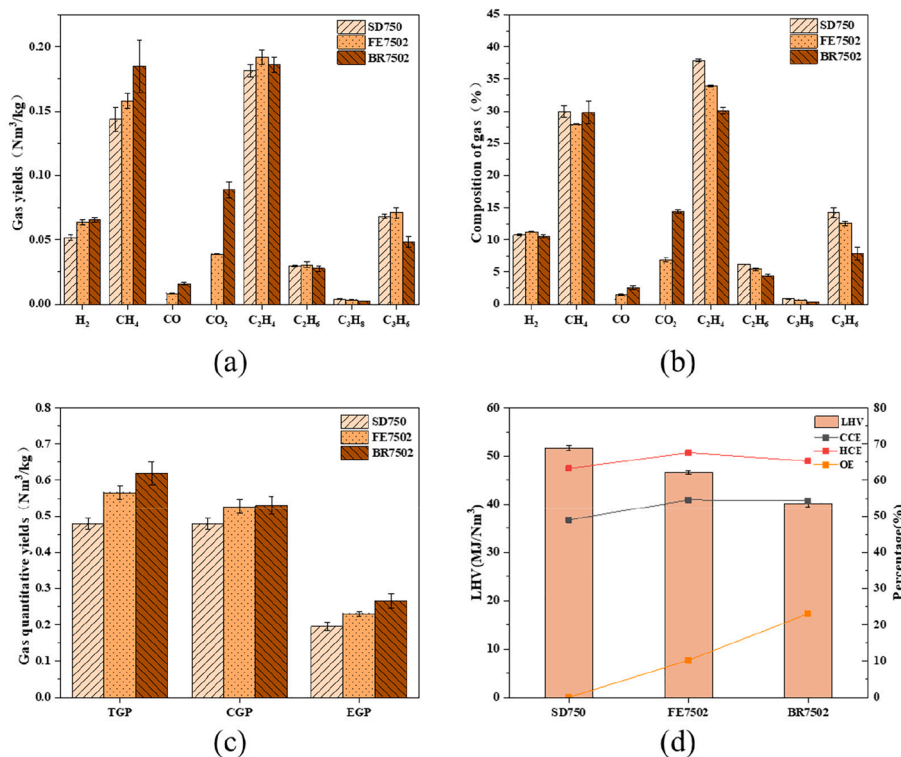


Fig. 2. Effects of oxygen carriers in the gasification process: (a) gas yields; (b) composition of fuel gas; (c) TGP, CGP, and EGP; and (d) LHV, CCE, HCE, and OE.

highest (37.913%), but declined to 30.070% after BR was added, with a decrease of 20%. C₃H₆ and C₂H₆ also showed some decline between the two groups. This confirms that the application of oxygen carriers promotes the conversion of C2-C3 to smaller molecules (H₂ and CH₄).

The TGP, CGP, and EGP shown in Fig. 2(c) indicate that the oxygen carrier can improve the gas production during the pyrolysis of PE. Even if CO₂ was deducted, the yields of combustible gas components of FE7502 and BR7502 were still higher than those of SD750. The lattice oxygen carried by the oxygen carriers is released during the reaction with the pyrolysis products of plastic at 750 °C. Oxidation breaks the long carbon chains and produces more gas-phase products. Oxygen carriers also oxidize macromolecular gases such as C₃H₈ and transform them into smaller molecules such as CH₄, CO, and CO₂. X. Chen et al. obtained similar results in their research on the gasification process of oxygen carriers and biomass[37].

Furthermore, as oxygen carriers oxidize parts of the original pyrolysis gas from PE, which is equivalent to conducting an insufficient combustion, some energy of the pyrolysis gas is released. Therefore, the LHV of the gases decreased from 51.729 MJ/Nm³ (SD750) to 46.602 MJ/Nm³ (FE7502) and 40.125 MJ/Nm³ (BR7502). The CCE and HCE of PE increased after the addition of oxygen carriers, which implies that more C and H in PE are converted into gas, and oxygen carriers promote the conversion of hydrogen and carbon elements of PE into the gas.

BR showed a stronger oxidation capacity than Fe₂O₃. The yields of both CO and CO₂ of BR7502 were higher than those of FE7502 under the same experimental conditions, reaching 0.016 Nm³/kg and 0.089 Nm³/kg, respectively. Moreover, the OE of BR7502 is almost twice that of FE7502, which implies that more oxygen is released by BR at 750 °C. This phenomenon may be caused by two factors: first, Fe₂O₃ sinters very easily at a high temperature, resulting in a decrease in its capacity to release oxygen[38]. The composition of the BR is considerably complex, and some inert components, such as Al₂O₃, can provide structural support for the active part and prevent sintering. Second, the alkali metal contained in BRs, such as Na, can also promote the diffusion of gas[34], which makes the reaction more complete.

The BR in Fig. 2(c) performs better than Fe₂O₃ and SD in TGP, CGP, and EGP. However, because of the strong oxidation, some hydrogen may be oxidized to water and cannot be detected, and some carbon may be excessively oxidized to CO₂, which explains why the HCE of BR7502 is slightly lower than that of the Fe₂O₃ group. The CCE of BR7502 is nearly the same as that of FE7502, although more CO₂ and CO are generated with the BR, which is probably due to the subsequent conversion of C₃H₆, C₃H₈, C₂H₆, and C₂H₄ to CO and CO₂.

3.4. Effect of temperature in the gasification process

The reaction results at different temperatures with SD and BR are shown in Fig. 3. The translucent histograms are the difference between the gas of BR and SD. They are applied to eliminate the effects of rising pyrolysis temperatures from 650 °C to 850 °C.

Fig. 3(a) shows the fuel gas yield. In the presence of BR, the production of small-molecule gas gradually increases with increasing temperature. The formation of CO is most sensitive to temperature and escalates from 0.003 Nm³/kg (650 °C) to 0.043 Nm³/kg (850 °C). The outputs of other small molecule gases (H₂, CH₄, and CO₂) also increase to varying degrees. Notably, the production of C₂H₄ increases initially and subsequently decreases, which may be attributed to the gradually enhanced oxidizability of BR with increasing temperature. Simultaneously, the other gases showed a downward trend in production as the temperature increased. The increasing yields of CO and CO₂ indicate that more oxygen migrates to the gas products at higher temperatures, and the OE also increases. This result suggests that the oxygen release capacity of BR increases with increasing temperature.

Compared with the H₂ yields of SD650 and SD750, the output of H₂ is higher with BR. However, the formation of H₂ was inhibited by BR at 850 °C. This is caused by the stronger oxidizability of BR at higher temperatures, resulting in the conversion of H₂ to H₂O. It can be seen from Fig. 3 (a) that the difference of CH₄ between BR8502 and SD850 is much lower than that between BR7502 and SD750. The addition of oxygen carrier can enhance the production of CH₄. But the gas

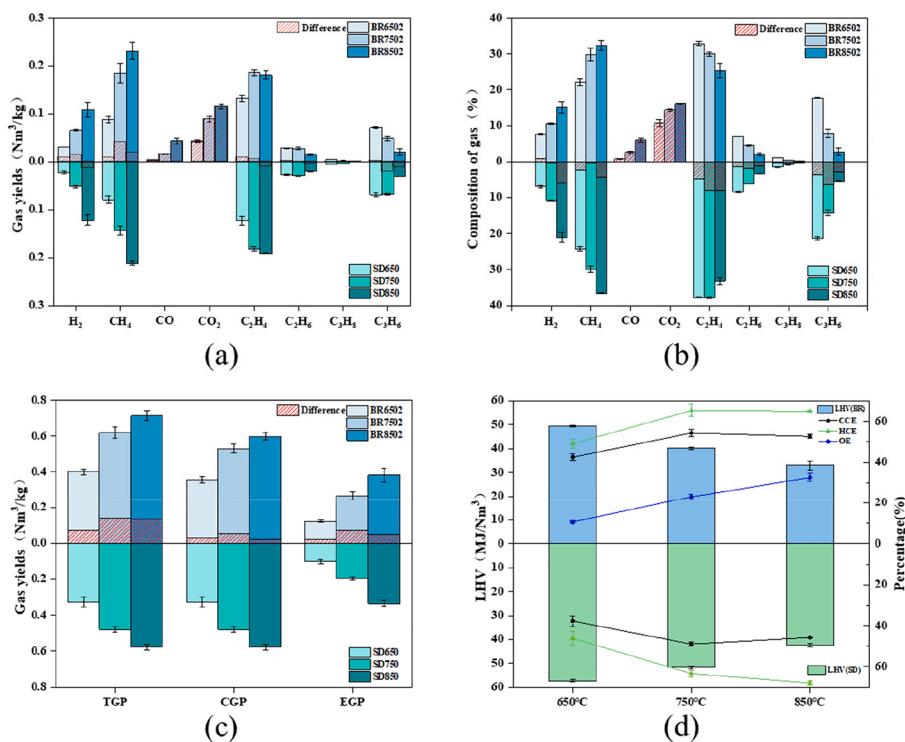


Fig. 3. Effects of temperature in the gasification process: (a) gas yields; (b) composition of fuel gas; (c) TGP, CGP, and EGP; and (d) LHV, CCE, HCE, and OE (mass ratio of plastic to oxygen carrier = 1:2).

production may also be oxidized by oxygen carrier. The rise of temperature promotes the oxygen release capacity of BR from 750 °C to 850 °C, some generated CH₄ may be also oxidized, but the promoted part is not oxidized completely. Thus, the difference of CH₄ in Fig. 3 (a) decreases when temperature is increased to 850 °C and the yield of CH₄ obtained at 750 °C was lower than that of CH₄ obtained at 850 °C. The enhanced oxygen release capacity of BR results in the decrease of H₂ yield and the decline of the difference of CH₄ at 850 °C. Moreover, the strong oxygen release capacity may also be the reason for the decrease in C₂H₄ at 850 °C. Therefore, lower temperatures lead to lower fuel gas yields, while higher temperatures may induce excessive oxidation of products and generate CO₂ and H₂O. The optimum conditions require a reasonable balance.

The distributions of the different components in the fuel gas are shown in Fig. 3(b). The proportion of most gases, except for CO and CO₂, was higher for the SD groups, which suggests that the spikes of CO and CO₂ result in an observable increase in TGP and a decrease in the percentage of individual gases. However, the promotion of BR at 850 °C decreases, which might result from the excessive oxidation of fuel gas by the oxygen carrier. Consequently, the enhancement in the reaction performance of BR owing to temperature is also limited. Although a higher pyrolysis temperature can increase the conversion of pyrolysis gas to small molecules, the addition of oxygen carriers can significantly promote the yields of H₂, CH₄, and CO.

Notably, the TGP, CGP, and EGP of the BR groups were higher than those of SD groups from 650 °C to 850 °C (Fig. 3(c)). This implies that the BR exhibits an improvement in gas production with a mass ratio of 1:2. The difference histograms also show that the BR has the most obvious promotion effect on plastic pyrolysis at 750 °C with a mass ratio of 1:2, and the highest TGP, CGP, and EGP differences were achieved.

The LHV, CCE, HCE, and OE are shown in Fig. 3(d). The LHV of the gas product decreased with increasing temperature. The decrease in LHV may be caused by the decomposition of C₃H₆ with a high calorific value and the formation of gases with low calorific value (H₂, CH₄, and CO). Meanwhile, the LHV of all the BR groups was lower because of the

oxidation of C₂H₄, C₂H₆, C₃H₆, and C₃H₈. All the HCE curves showed an upward trend. However, as mentioned before, hydrogen in the BR groups may be partly oxidized into undetectable water; thus, the HCE in the BR group was 2.972% lower than that of the SD group at 850 °C. The CCE curves in Fig. 3(d) increase initially and subsequently decrease slightly. In the tests with BR, CCE increased by 23.814% when the temperature increased from 650 °C to 850 °C. Correspondingly, the CCE of the three SD groups increased from 37.709% (650 °C) to 45.733% (850 °C). Apparently, BR added as an oxygen carrier increases the CCE under all three conditions. The decrease in CCE at 850 °C demonstrates that the carbon tends to be deposited at the surface of BR, resulting in lower carbon conversion efficiency.

3.5. Effects of mass ratio in the gasification progress

The effects of the mass ratio of oxygen carriers at 750 °C are shown in Fig. 4. SD was applied to maintain the same resistance time in section 2. When the mass ratio was maintained at 1:2, the generation of small molecule gases, such as H₂, CH₄, CO, and CO₂, is promoted. The yields of the larger gas molecules (such as C₃H₆) were inhibited because of oxidation by the BR as before. However, when the mass ratio was increased to 1:4, the H₂ yield decreased to 0.043 Nm³/kg (BR7504), which was less than that of SD750; this may be caused by the oxidation of the superfluous BR. The output of CO decreased slightly from 0.016 Nm³/kg (BR7502) to 0.014 Nm³/kg (BR7504) with the addition of BR. The production of CH₄, C₂H₆, and C₃H₆ in BR7504 was almost the same as that of BR7502. This reveals that the carbon in heavy products tends to metastasize to the gas with a higher oxygen carrier ratio. As for CO₂, the output increased by 87.460% after doubling the mass ratio. Thus, the yields of combustible gas components decline when more oxygen carriers are applied. Therefore, a proper ratio of BR to PE is crucial for high-value conversion.

Fig. 4(b) is similar to Fig. 4(a), wherein nearly all the proportions of gases are reduced after increasing the mass of BR, while the yield of CO₂ increases from 14.338% (BR7502) to 24.934% (BR7504). The rapid

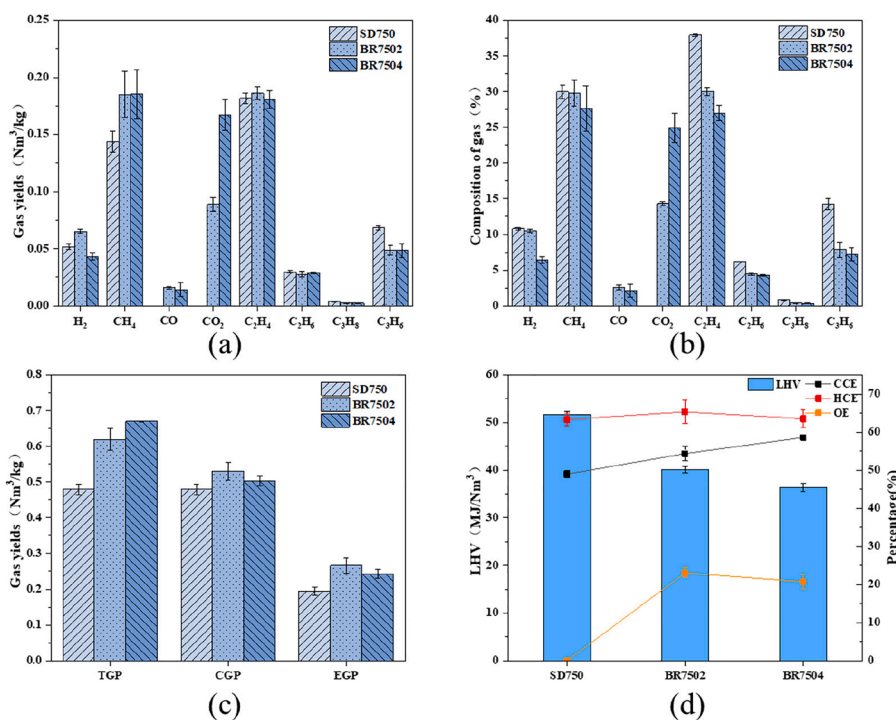


Fig. 4. Effects of mass ratio in the gasification process: (a) gas yields; (b) composition of fuel gas; (c) TGP, CGP, and EGP; and (d) LHV, CCE, HCE, and OE (experiment temperature = 750 °C).

increase in the output of CO₂ and excessive oxidation of combustible gas by BR resulted in a decrease in the proportions of other gas components. However, the proportions of CH₄, C₂H₄, and C₃H₆ decreased while their yields remained the same. A possible explanation is that the total gas output increased, but the yields showed no obvious change.

As shown in Fig. 4(c), both CGP and EGP decreased with higher BR ratios, while TGP increased. The enhancement effect of BR on the gas quality of BR7502 was inhibited by BR7504. Notably, the total gas output is enhanced by excessive BR because of the formation of CO₂. Meanwhile, a considerable amount of H₂ may be oxidized into water, decreasing the proportion of combustible components in the fuel gas. Therefore, a higher ratio of oxygen carriers is detrimental to the quality and yield of the fuel gas.

As shown in Fig. 4(d), the LHV decreased from 51.729 MJ/Nm³ (SD750) to 40.125 (BR7502) and 36.340 MJ/Nm³ (BR7504) because of the gradually enhanced oxygen release capacity of BR. This is also the reason for the decline in HCE from 65.338% for BR7502 to 63.513% for BR7504. The CCE increased from 48.944% under SD750 to 58.589% under BR7504, which indicates that more BR can promote the conversion of carbon in heavy products to gaseous products. Despite the increase in the amount of oxygen in the gas of BR7504, the BR also increases. The amount of effective oxygen in the gas increases insignificantly compared to twice the oxygen input. Consequently, OE decreases from 23.061% to 20.722%.

Considering the influence of temperature in section 3.2, both higher temperature and more BR addition can improve the oxygen release capacity of BR. An overly strong oxygen release capacity does not produce more combustible gas but will lead to excessive oxidation of the gas product. The degree of reduction in BR itself may also be affected. Turning points exist in the temperature and mass ratios; in these experiments, the turning point of temperature was 750 °C and that of the mass ratio was 1:2.

3.6. Effects of reactor arrangement in the gasification process

To improve the EGP and reduce the production of CO₂, an additional

reaction section was applied on the basis of the previous system. This is intended to facilitate the dry reforming reaction of CO₂ and CH₄ to produce more CO and H₂. The influence of the third-stage reactor on the fuel gas yield and quality is shown in Fig. 5. Fe₂O₃ is proven to be an effective catalyst for dry reforming reactions at high temperatures (900 °C) [39]. Therefore, the reactant in the second reactor was also BR, and the reaction temperature was set to 900 °C. The mass ratio of BR in the second tube was 1:1 to prevent excessive oxidation.

The gas yields in Fig. 5(a) show a significant difference among BR2, BR8502, and SD850. For BR2, the H₂ content was almost twice that of BR8502, reaching 0.257 Nm³/kg. The substantial increase in H₂ may be caused by the combination of the CO₂ reforming reaction and carbon deposition at high temperatures. Moreover, the yields of both CO and CH₄ of BR2 were higher than those of BR8502. As for CH₄, the yield slightly increased from 0.231 to 0.242 Nm³/kg, which can be attributed to the decomposition of macromolecular gases. The yield of CO increased from 0.043 Nm³/kg to 0.148 Nm³/kg, but that of CO₂ decreased by 0.004 Nm³/kg. This may have resulted from the reforming reactions of CO₂ and CH₄. For BR2, the yield of C₂H₄ sharply drops to 0.010 Nm³/kg, and the production of C₂H₆, C₃H₈, and C₃H₆ decreased significantly. This demonstrates that C₂ + may be converted into solid carbon, CO, and H₂.

As shown in Fig. 5(b), the total yields of H₂, CH₄, CO, and CO₂ were 98.469%. The proportion of effective syngas (H₂, CH₄, and CO) accounts for 83.960% of the gas product. To eliminate the contained CO₂, the gas product could be purged with an alkaline solution, and the effective syngas ratio would reach 98.201%. Consequently, the quality of the fuel gas is impaired by excessive oxidation, which indicates that an inhibitor is required to restrain the oxygen release capability of BR and maintain the catalytic activity for the dry reforming reaction.

As shown in Fig. 5(c) and (d), TGP, CGP, and EGP are promoted for the third-stage reaction. In particular, the EGP of BR2 increased by 69%. In Fig. 5(d), the LHV of BR2 is the lowest, which results from the extremely low contents of C₂H₄, C₂H₆, C₃H₈, and C₃H₆. CCE, HCE, and OE in Fig. 5(d) decline for different reasons. The decrease in CCE was caused by the carbon deposition in the third stage at 900 °C. The lower

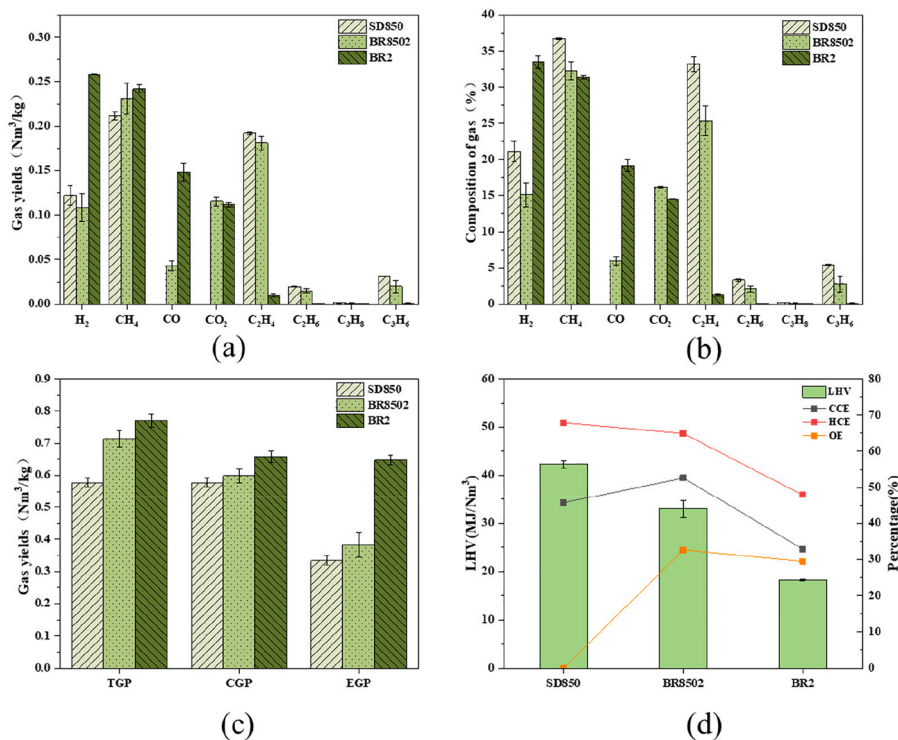


Fig. 5. Effects of the third-stage reactor in the gasification process: (a) gas yields; (b) composition of fuel gas; (c) TGP, CGP, and EGP; and (d) LHV, CCE, HCE, and OE.

HCE can be interpreted as the oxidation of H₂ to water in the third stage. Although more oxygen is transferred into the gas production of BR2, the amount of lattice oxygen added to the experiment also increases owing to the increase in the mass of BR. As the heavy products are condensed after the first reactor, only a portion of the products participate in the reaction with BR in stage 3. Therefore, the OE of BR2 was lower than that of BR7502.

3.7. Characterization of the materials

Table 3 presents the N₂ adsorption/desorption isotherms of fresh BR and Fe₂O₃. After simple treatment, fresh BR has a larger BET surface than Fe₂O₃, and its pore volume is smaller, which corresponds to the stronger oxidation capacity of BR described in section 3.1. This is probably because the inert substances contained in BR provide structural support.

The XRD patterns of the washed, fresh, and used BRs are illustrated in Fig. 6. Washed BR represents the BR after pretreatment with deionized water, fresh BR indicates that BR has been calcined at 900 °C, and used BR is derived from BR8504. Compared with washed BR, the phases in the fresh BR are reduced, mainly including hematite (Fe₂O₃), gehlenite (Ca₂Al₂SiO₇), iron titanium oxide (Fe₉TiO₁₅), and aluminosilicate (NaAlSiO₄), which are no longer detected. After gasification, the Fe₂O₃ peak disappeared and was replaced by magnetite (Fe₃O₄). This indicates that oxygen in the BR was not fully utilized in the reaction. However, because of the magnetic characteristics of magnetite (Fe₃O₄), the BR after gasification can be obtained by magnetic separation for further utilization. The inert matrix, such as Ca₂Al₂SiO₇, is maintained after the

Table 3
The BET surface area and pore volume of fresh BR and Fe₂O₃.

Materials	BET surface area (m ² /g)	Pore volume (cm ³ /g)
Fresh BR	4.047	9.670 × 10 ⁻³
Fe ₂ O ₃	3.721	10.720 × 10 ⁻³

reaction, provides support for Fe₂O₃ throughout the process. The reason for the absence of lower valence iron may be the insufficient reduction in BR.

Fig. 7 shows the microscopic images of washed, fresh, and used BRs. Before calcination, the micro-surface of the BR presents a state of random accumulation, wherein flaky and rod-shaped disordered clusters with different sizes and shapes gather together. After calcination at 900 °C for 2 h, BR is relatively uniform throughout the whole surface. Some small cracks and holes appear on the melted surface. Although some blocked or cracked holes are found on the surface of used BR after the reaction, the overall structure is still relatively complete.

4. Conclusion

The feasibility of converting waste polyethylene into high-quality fuel gas using bauxite residue as an oxygen carrier was experimentally studied. The main findings are as follows.

- (1) It is an effective way to produce fuel gas through polyethylene gasification using bauxite residue as an oxygen carrier. A maximum of 0.771 Nm³ of fuel gas was produced per kilogram of polyethylene in this study. The lower heating value of the fuel gas was 18.245 MJ/Nm³. Under the same conditions, the oxygen efficiency of the bauxite residue was more than 100% higher than that of Fe₂O₃.
- (2) Temperature had a significant effect on the reaction activity of the bauxite residue. With the increase in temperature from 650 to 850 °C, the total gas production ranged from 0.400 Nm³/kg to 0.714 Nm³/kg. The lower heating value of the fuel gas decreased from 49.466 MJ/Nm³ to 32.972 MJ/Nm³. The oxygen release capacity of the bauxite residue was also enhanced. The contents of CO and CO₂ gradually increased to 0.043 and 0.116 Nm³/kg, respectively. At a certain mass ratio, the excessive temperature might weaken the promotion effect on gas production and produce a large amount of CO₂.

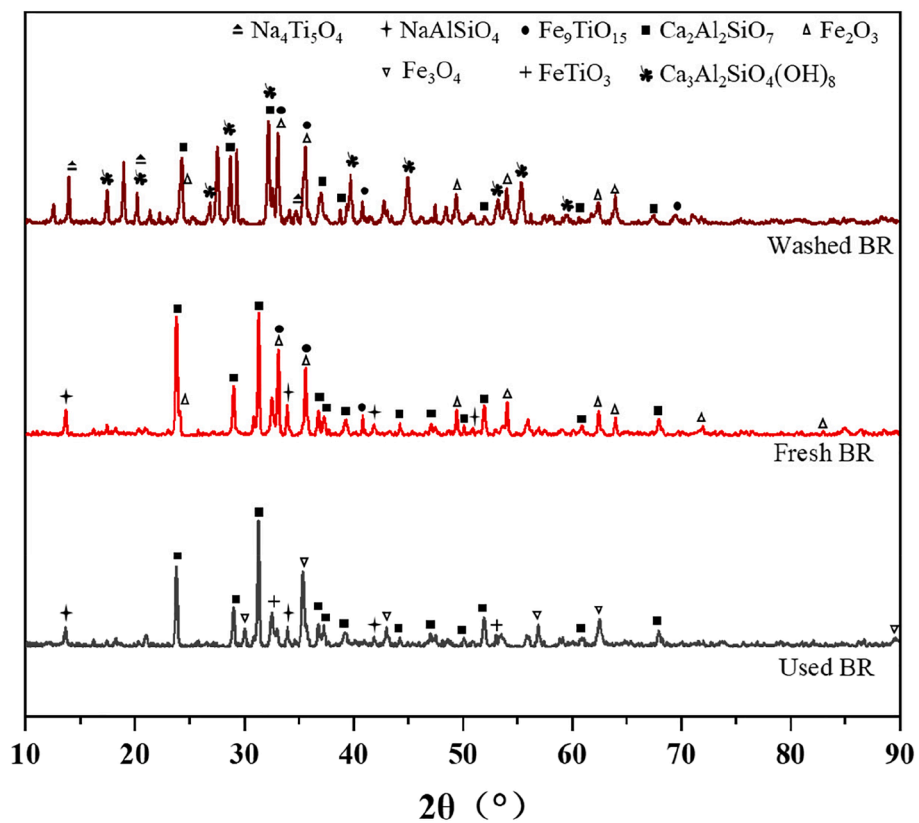


Fig. 6. XRD patterns of washed BR, fresh BR, and used BR.

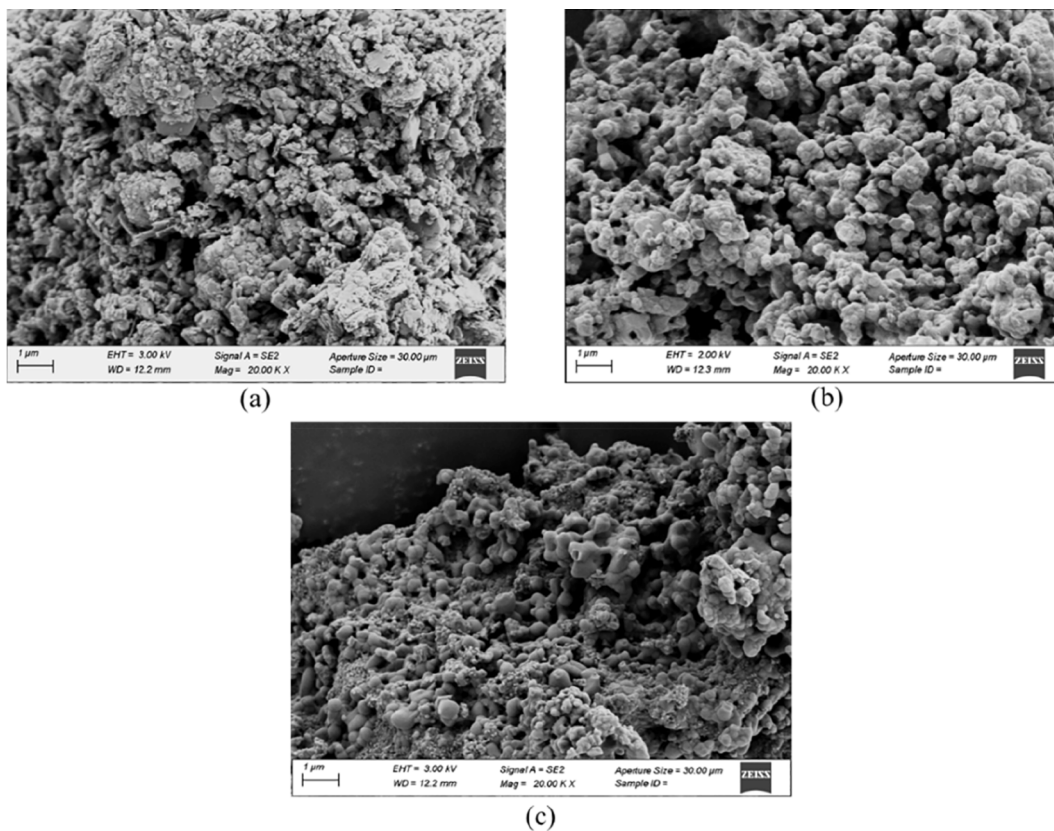


Fig. 7. SEM images of (a) washed BR, (b) fresh BR, and (c) used BR.

- (3) With the increasing mass ratio, bauxite residue initially promoted and subsequently inhibited the gas products. Excessive bauxite residue would not only lead to the full oxidation of gas products but would also reduce the utilization efficiency of oxygen in the bauxite residue. A mass ratio of 1:2 at 750 °C yielded the highest combustible gas production (0.531 Nm³/kg).
- (4) The effective syngas production of BR2 increased by nearly 70%, from 0.383 to 0.647 Nm³/kg of BR8502. Synchronously, gas products with a proportion of 83.960% for effective syngas (H₂, CH₄, and CO) were also collected in the third-stage method.
- (5) After the reaction, some iron in the bauxite residue was converted into Fe₃O₄, which could contribute to Fe recovery through magnetic separation.

CRedit authorship contribution statement

Xudong Du: Conceptualization, Methodology, Writing – original draft. **Jun Wang:** Data curation. **Jiaying Song:** Visualization. **Yuhan Pan:** Investigation. **Jingyuan Sima:** Resources. **Chenxi Zhu:** Formal analysis. **Huaping Gao:** Resources. **Linlin Guo:** Validation. **Jie Zhang:** Validation. **Qunxing Huang:** Writing – review & editing, Supervision, Project administration.

Declaration of Competing Interest

The authors declare that they have no known competing financial interests or personal relationships that could have appeared to influence the work reported in this paper.

Acknowledgments

The authors would like to gratefully acknowledge the National Natural Science Foundation of China (52076190), Ecological civilization plan of Zhejiang University, Zhejiang Province Science and Technology Program (2022C03082).

Appendix A. Supplementary data

Supplementary data to this article can be found online at <https://doi.org/10.1016/j.fuel.2022.123878>.

References

- [1] Wong SL, Ngadi N, Abdullah TAT, Inuwa IM. Current state and future prospects of plastic waste as source of fuel: A review. *Renew Sustain Energy Rev* 2015;50:1167–80.
- [2] Abbas-Abadi MS. The effect of process and structural parameters on the stability, thermo-mechanical and thermal degradation of polymers with hydrocarbon skeleton containing PE, PP, PS, PVC, NR, PBR and SBR. *J Therm Anal Calorim* 2021;143(4):2867–82.
- [3] PLASTICSEUROPE, Plastics-the Facts 2019. An analysis of European plastics production, demand and waste data. Brussels: PlasticsEurope; 2019.
- [4] Al-Salem SM, Lettieri P, Baeyens J. The valorization of plastic solid waste (PSW) by primary to quaternary routes: From re-use to energy and chemicals. *Prog Energy Combust Sci* 2010;36(1):103–29.
- [5] Soares J, Miguel I, Venâncio C, Lopes I, Oliveira M. Public views on plastic pollution: Knowledge, perceived impacts, and pro-environmental behaviours. *J Hazard Mater* 2021;412:125227. <https://doi.org/10.1016/j.jhazmat.2021.125227>.
- [6] Teuten EL, Saquing JM, Knappe DRU, Barlaz MA, Jonsson S, Björn A, et al. Transport and release of chemicals from plastics to the environment and to wildlife. *Philos Trans R Soc Lond B Biol Sci* 2009;364(1526):2027–45.
- [7] Zhang F, Zhao Y, Wang D, Yan M, Zhang J, Zhang P, et al. Current technologies for plastic waste treatment: A review. *J Cleaner Prod* 2021;282:124523. <https://doi.org/10.1016/j.jclepro.2020.124523>.
- [8] Ji G, Yao JG, Clough PT, da Costa JCD, Anthony EJ, Fennell PS, et al. Enhanced hydrogen production from thermochemical processes. *Energy Environ Sci* 2018;11(10):2647–72.
- [9] Sarafraz MM, Jafarian M, Arjomandi M, Nathan GJ. Potential use of liquid metal oxides for chemical looping gasification: A thermodynamic assessment. *Appl Energy* 2017;195:702–12.
- [10] Di Z, Cao Y, Yang F, Cheng F, Zhang K. Studies on steel slag as an oxygen carrier for chemical looping combustion. *Fuel* 2018;226:618–26.
- [11] Hammache S, Means N, Burgess W, Howard B, Smith M. Investigation of low-cost oxygen carriers for chemical looping combustion at high temperature. *Fuel* 2020;273:117746. <https://doi.org/10.1016/j.fuel.2020.117746>.
- [12] Gu Z, Zhang L, Lu C, Qing S, Li K. Enhanced performance of copper ore oxygen carrier by red mud modification for chemical looping combustion. *Appl Energy* 2020;277:115590. <https://doi.org/10.1016/j.apenergy.2020.115590>.
- [13] Hu Z, Miao Z, Wu J, Jiang E. Nickel-iron modified natural ore oxygen carriers for chemical looping steam methane reforming to produce hydrogen. *Int J Hydrogen Energy* 2021;46(80):39700–18.
- [14] Yu Z, Yang Y, Yang S, Zhang Q, Zhao J, Fang Y, et al. Iron-based oxygen carriers in chemical looping conversions: A review. *Carbon Resour Convers* 2019;2(1):23–34.
- [15] Feng Y, Wang N, Guo X. Influence mechanism of supports on the reactivity of Ni-based oxygen carriers for chemical looping reforming: A DFT study. *Fuel* 2018;229:88–94.
- [16] Tijani MM, Aqsha A, Mahinpey N. Synthesis and study of metal-based oxygen carriers (Cu Co, Fe, Ni) and their interaction with supported metal oxides (Al₂O₃, CeO₂, TiO₂, ZrO₂) in a chemical looping combustion system. *Energy* 2017;138:873–82.
- [17] Costa TR, Gayán P, Abad A, García-Labiano F, de Diego LF, Melo DMA, et al. Mn-based oxygen carriers prepared by impregnation for Chemical Looping Combustion with diverse fuels. *Fuel Process Technol* 2018;178:236–50.
- [18] Abad A, Mattisson T, Lyngfelt A, Ryden M. Chemical-looping combustion in a 300W continuously operating reactor system using a manganese-based oxygen carrier. *Fuel* 2006;85(9):1174–85.
- [19] Idziak K, Czakiert T, Krzywanski J, Zylka A, Kozłowska M, Nowak W. Safety and environmental reasons for the use of Ni-, Co-, Cu-, Mn- and Fe-based oxygen carriers in CLC/CLOU applications: An overview. *Fuel* 2020;268:117245. <https://doi.org/10.1016/j.fuel.2020.117245>.
- [20] Cuadrat A, Abad A, García-Labiano F, Gayán P, de Diego LF, Adán J. The use of ilmenite as oxygen-carrier in a 500Wth Chemical-Looping Coal Combustion unit. *Int J Greenhouse Gas Control* 2011;5(6):1630–42.
- [21] Zhang S, Gu H, Zhao J, Shen L, Wang L. Development of iron ore oxygen carrier modified with biomass ash for chemical looping combustion. *Energy* 2019;186:115893. <https://doi.org/10.1016/j.energy.2019.115893>.
- [22] Liu T, Yu Z, Li G, Guo S, Shan J, Li C, et al. Performance of potassium-modified Fe₂O₃/Al₂O₃ oxygen Carrier in coal-direct chemical looping hydrogen generation. *Int J Hydrogen Energy* 2018;43(42):19384–95.
- [23] Bhavsar S, Najera M, Veser G. Chemical Looping Dry Reforming as Novel, Intensified Process for CO₂ Activation. *Chem Eng Technol* 2012;35(7):1281–90.
- [24] Ku Y, Liu Y-C, Chiu P-C, Kuo Y-L, Tseng Y-H. Mechanism of Fe₂TiO₅ as oxygen carrier for chemical looping process and evaluation for hydrogen generation. *Ceram Int* 2014;40(3):4599–605.
- [25] Agrawal S, Dhawan N. Evaluation of red mud as a polymetallic source – A review. *Miner Eng* 2021;171:107084. <https://doi.org/10.1016/j.mineng.2021.107084>.
- [26] Rai S, Bahadure S, Chaddha MJ, Agnihotri A. Disposal Practices and Utilization of Red Mud (Bauxite Residue): a Review in Indian Context and Abroad. *J Sustain Metall* 2020;6(1):1–8.
- [27] Wang Li, Sun N, Tang H, Sun W. A Review on Comprehensive Utilization of Red Mud and Prospect Analysis. *Minerals* 2019;9(6):362. <https://doi.org/10.3390/min9060362>.
- [28] Zhang J, Yao Z, Wang K, Wang F, Jiang H, Liang M, et al. Sustainable utilization of bauxite residue (Red Mud) as a road material in pavements: A critical review. *Constr Build Mater* 2021;270:121419. <https://doi.org/10.1016/j.conbuildmat.2020.121419>.
- [29] Kumar A, Saravanan TJ, Bisht K, Kabeer KISA. A review on the utilization of red mud for the production of geopolymer and alkali activated concrete. *Constr Build Mater* 2021;302:124170. <https://doi.org/10.1016/j.conbuildmat.2021.124170>.
- [30] Li S, Pan J, Zhu D, Guo Z, Shi Y, Dong T, et al. A new route for separation and recovery of Fe. *Resour Conserv Recycl* 2021;168:105314. <https://doi.org/10.1016/j.resconrec.2020.105314>.
- [31] Carneiro J, Tobaldi DM, Capela MN, Novais RM, Seabra MP, Labrincha JA. Synthesis of ceramic pigments from industrial wastes: Red mud and electroplating sludge. *Waste Manag* 2018;80:371–8.
- [32] Lin S, Gu Z, Zhu X, Wei Y, Long Y, Yang K, et al. Synergy of red mud oxygen carrier with MgO and NiO for enhanced chemical-looping combustion. *Energy* 2020;197:117202. <https://doi.org/10.1016/j.energy.2020.117202>.
- [33] López A, de Marco I, Caballero BM, Laresgoiti MF, Adrados A, Aranzabal A. Catalytic pyrolysis of plastic wastes with two different types of catalysts: ZSM-5 zeolite and Red Mud. *Appl Catal B* 2011;104(3–4):211–9.
- [34] Bao J, Chen L, Liu F, Fan Z, Nikolic HS, Liu K. Evaluating the Effect of Inert Supports and Alkali Sodium on the Performance of Red Mud Oxygen Carrier in Chemical Looping Combustion. *Ind Eng Chem Res* 2016;55(29):8046–57.
- [35] Mendiara T, de Diego LF, García-Labiano F, Gayán P, Abad A, Adán J. Behaviour of a bauxite waste material as oxygen carrier in a 500 Wth CLC unit with coal. *Int J Greenhouse Gas Control* 2013;17:170–82.
- [36] Abad A, Mendiara T, Gayán P, García-Labiano F, de Diego LF, Bueno JA, et al. Comparative Evaluation of the Performance of Coal Combustion in 0.5 and 50 kWth Chemical Looping Combustion Units with Ilmenite, Redmud or Iron Ore as Oxygen Carrier. *Energy Procedia* 2017;114:285–301.

- [37] Shen X, Yan F, Zhang Z, Li C, Zhao S, Zhang Z. Enhanced and environment-friendly chemical looping gasification of crop straw using red mud as a sinter-resistant oxygen carrier. *Waste Manag* 2021;121:354–64.
- [38] Zeng J, Xiao R, Zhang S, Zhang H, Zeng D, Qiu Yu, et al. Identifying iron-based oxygen carrier reduction during biomass chemical looping gasification on a thermogravimetric fixed-bed reactor. *Appl Energy* 2018;229:404–12.
- [39] Kang D, Lee M, Lim HS, Lee JW. Chemical looping partial oxidation of methane with CO₂ utilization on the ceria-enhanced mesoporous Fe₂O₃ oxygen carrier. *Fuel* 2018;215:787–98.